Splay-bend elasticity of a nematic liquid crystal with T-shaped molecules

P. Sathyanarayana,[1] M. C. Varia,[2] A. K. Prajapati,[2] B. Kundu,[1,*] V. S. S. Sastry,[1] and S. Dhara[1,†]

[1]*School of Physics, University of Hyderabad, Hyderabad 500046, India*
[2]*Department of Applied Chemistry, Faculty of Technology and Engineering, M. S. University of Baroda,*
Vadodara 390001, India

We measured the splay (K_{11}) and bend (K_{33}) elastic constants in the nematic phase of a liquid crystal with T-shaped molecules. We find that the ratio, $K_{33}/K_{11} \simeq 1$ in the entire nematic range except very close to the nematic to Sm-A (SN) transition. *Both* K_{33} and K_{11} show pretransitional divergence as the SN transition is approached from higher temperature. The ratio, K_{33}/K_{11} suggests that the length (L) to effective width (D) ratio (i.e., L/D) is significantly smaller due to the presence of long and flexible lateral group, compared to that of rigid rodlike molecules. It is argued that apart from the extra contribution to the elasticity the long and flexible lateral group also has a significant contribution to the suppression of the splay fluctuations in the onset of smectic short-range fluctuation. The structure of the Sm-A phase is investigated by using small angle x-ray diffraction, and a possible arrangement of the molecules in the Sm-A layer is proposed.

Interest in the synthesis and physical characterization of liquid crystals with chemical structure similar to the shapes of many English letters such as V, T, H, W has increased after the discovery of electro-optical switching in bent-core liquid crystals [1–3]. The structure-property relationship of such unconventional liquid crystals has always been interesting from both technological and fundamental points of view. It is observed that the physical properties and, in particular electro-optical responses, in these unconventional liquid crystals are very different compared with the calamitic liquid crystals, and the molecular shape has significant effect on phase structure and macroscopic physical properties [4]. For investigating the structure-property relation, nematic phase (N) has been chosen due to its simplicity. There are many interesting physical properties reported in the nematic phase of bent-core liquid crystals among the unconventional liquid crystal molecules mentioned above. It has been found that bent-core nematic has a number of extraordinary properties such as the sign inversion of elastic anisotropy ($K_{33} - K_{11}$) [5], unusual electroconvection [6], giant flexoelectricity [7], and large viscosity [8]. In this paper we report measurement of order parameter, splay, and bend elastic constants of a liquid crystal comprising of T-shaped molecules. These are found to be significantly different from the conventional calamitic and bent-core liquid crystals. Further, from the x-ray diffraction measurements we propose a possible orientation of these T-shaped molecules in the Sm-A layers.

The compound used in the present study was synthesized in our laboratory and the details will be reported elsewhere. The chemical structure of the compound is shown in Fig. 2(a). It has the following phase sequence: Cr 90 °C Sm-A 108 °C N 128 °C I. Planar aligned cells were prepared by

using two glass plates coated with indium tin-oxide. The plates were treated with polyimide and cured at 180 °C for one hour and rubbed antiparallel to prepare cells with planar alignment. For homeotropic cells, JALS-204 was used and cured at 200 °C for 1 h. Typical cell thickness used for the experiments was $d \sim 5$ μm. The parallel ($\epsilon_{\parallel}$) and perpendicular ($\epsilon_{\perp}$) components of the dielectric constant were measured as a function of temperature in homeotropic and planar cells, respectively, with a LCR meter (Agilent 4980A) at 4111 Hz, applying a voltage of 0.3 V. The optical phase retardation was measured by using the phase modulation technique [9]. The setup comprises a Helium-Neon laser ($\lambda = 632.8$ nm), photoelastic modulator (PEM-100) and a lock-in amplifier (SR-830). The retardation and sample capacitance were measured simultaneously as functions of temperature and voltage up to 20 V in steps ranging from 0.05 V to 0.5 V. The x-ray diffraction measurements were made using Cu K_{α} radiation from a rotating anode. The splay elastic constant K_{11} was measured directly from the Freedericksz threshold voltage (V_{th}) of the voltage dependent retardation data using the equation $K_{11} = \epsilon_o \Delta \epsilon (V_{th}/\pi)^2$, where $\Delta \epsilon (= \epsilon_{\parallel} - \epsilon_{\perp})$ is the dielectric anisotropy. The voltage dependent optical phase difference (δ), and voltages above the threshold voltage V_{th}, are given by following parametric equations [10,11]:
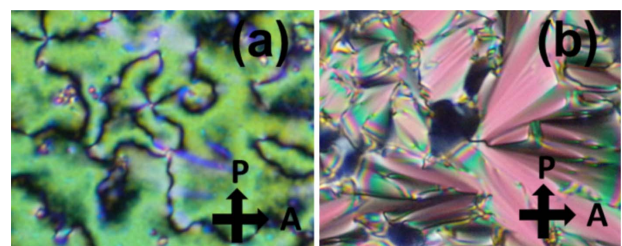

FIG. 1. (Color online) (a) Schlieren texture in nematic phase (at 123 °C) and (b) Focal conic texture in Sm-A phase (at 103 °C).

*Present address: Liquid Crystal Institute, Tokyo University of Science, Yamaguchi, Japan.

†Corresponding author; sdsp@uohyd.ernet.in

$$\frac{V}{V_{th}} = \frac{2}{\pi}\sqrt{1 + \gamma \sin^2(\phi_m)} \int_0^{\pi/2} \sqrt{\frac{1 + \kappa \sin^2(\phi_m)\sin^2(\psi)}{[1 + \gamma \sin^2(\phi_m)\sin^2(\psi)][1 - \sin^2(\phi_m)\sin^2(\psi)]}} d\psi, \tag{1}$$

$$\delta = 2\pi \frac{n_e d}{\lambda} \times \left\{ \frac{\displaystyle\int_0^{\pi/2} \sqrt{\frac{[1 + \gamma \sin^2(\phi_m)\sin^2(\psi)][1 + \kappa \sin^2(\phi_m)\sin^2(\psi)]}{[1 - \sin^2(\phi_m)\sin^2(\psi)][1 + \nu \sin^2(\phi_m)\sin^2(\psi)]}} d\psi}{\displaystyle\int_0^{\pi/2} \sqrt{\frac{[1 + \gamma \sin^2(\phi_m)\sin^2(\psi)][1 + \kappa \sin^2(\phi_m)\sin^2(\psi)]}{[1 - \sin^2(\phi_m)\sin^2(\psi)]}} d\psi} - \frac{n_o}{n_e} \right\}, \tag{2}$$

where d is the cell thickness, ϕ_m is the tilt angle at the middle of the cell and the other terms of the reduced quantities are: $\gamma = \frac{\epsilon_\parallel}{\epsilon_\perp} - 1$, $\kappa = \frac{K_{33}}{K_{11}} - 1$, $\nu = \frac{n_e^2}{n_o^2} - 1$, $\sin(\phi) = \sin(\phi_m)\sin(\psi)$. The sample retardation at higher voltages are fitted to the above equations by an iterative procedure to get the bend elastic constant K_{33} [10,11].

A typical schlieren texture in the nematic phase at 123 °C and a focal conic texture in the Sm-*A* phase at 103 °C are shown in Fig. 1. A uniform planar alignment of the director ($\hat{n}$) is obtained in rubbed cells. The variation of birefringence (Δn) in the N and the Sm-*A* phase as a function of temperature is shown in Fig. 2(a). Δn develops sharply at the NI phase transition as expected and gradually increases as the temperature decreases in the N phase. A significant increase in Δn is also observed in the Sm-*A* phase (below 108 °C). The temperature dependent Δn in N liquid crystals can be

FIG. 2. (Color online) (a) Variation of birefringence (Δn) and order parameter (S) as a function of temperature. Chemical structure and the energy minimized structure obtained from quantum chemical calculations using GAUSSIAN-03 (inset). (b) Variation of parallel ($\epsilon_\parallel$) and perpendicular ($\epsilon_\perp$) components of the dielectric constant and the dielectric anisotropy ($\Delta\epsilon$) as a function of temperature.

approximated by the formula $\Delta n = \Delta n_o (1 - T/T^*)^\beta$, where T^* and β are the adjustable fit parameters and Δn_o is the birefringence of the perfectly aligned sample. The equation fits well in the entire nematic range with fit parameters $\Delta n_o = 0.31$ and $\beta = 0.21$. The order parameter S was estimated using the relation $S = \Delta n / \Delta n_o$. The temperature variation of the calculated order parameter is also shown in Fig. 2(a). The jump in the order parameter at the NI transition was 0.25 and it increases to 0.65 (at 95 °C) with a significant increase $\Delta S_{SN} \sim 0.06$ (at 107 °C) in the Sm-*A* phase. There have been many experimental and theoretical studies on the N to Sm-*A* (SN) transition in compounds with rodlike molecules. The coupling between the smectic order parameter ψ and the fluctuations in the nematic order parameter S can cause a crossover toward a tricritical point leading to a first order transition as the McMillan parameter $\alpha (= T_{SN}/T_{NI})$ approaches 1 [12]. The theoretical value of α for the crossover to the tricritical point is $\alpha \sim 0.83$. However, the experimental value of α is not universal and is slightly higher [13], and it also depends on the type of the Sm-*A* phase [14,15]. The value of α for the present compound is 0.95 and is well above the tricritical point value. The large value of ΔS_{SN}(~ 0.06) in addition to large α suggests that the present SN transition is first order in nature. A small increase in S in the SN transition is also known in many other calamitic liquid crystals such as 8OCB (4-octyloxy 4′-cyanobiphenyl) [11], 8CB (4-octyl-4′-cyanobiphenyl) [10] and in some banana shaped compounds [5]. In the case of 8CB the jump in the order parameter ΔS_{SN} is ~ 0.01 and the SN transition is considered to be a weakly first order [16]. In the present compound ΔS_{SN} (~ 0.06) is much larger than that of 8CB. We also measured the enthalpies of NI (ΔH_{NI}) and NS transitions (ΔH_{SN}) using a differential scanning calorimeter. They are $\Delta H_{NI} = 2.0$ kJ/mol and $\Delta H_{SN} = 1.6$ kJ/mol, respectively. Thus enthalpies of both these transitions are *comparable* for present compound whereas ΔH_{SN} is ~ 11 and ~ 22 times smaller than ΔH_{NI} in cases of 8CB and 8OCB, respectively [17]. The large values of ΔS_{SN} and enthalpy (ΔH_{SN}) further support first order nature of the SN transition.

The temperature variation of parallel ($\epsilon_\parallel$) and perpendicular ($\epsilon_\perp$) components of the dielectric constant is shown in Fig. 2(b). The dielectric anisotropy is small and positive ($\Delta\epsilon = 0.9$ at $T = 115$ °C) in the N phase, and reduces in the Sm-*A* phase. The temperature dependent dielectric anisotropy is interpreted on the basis of the role of permanent dipoles and the molecular shape. The molecules have both
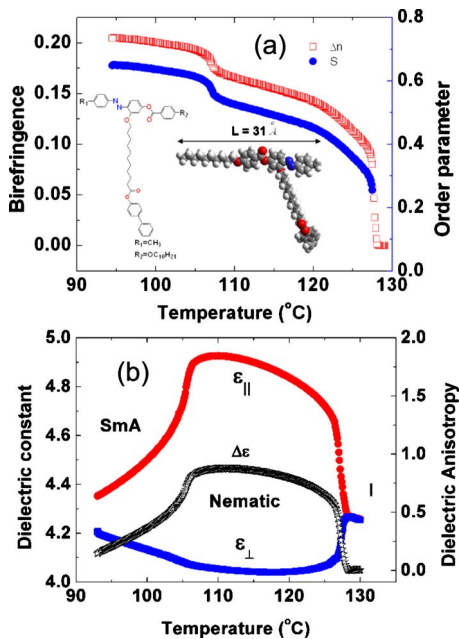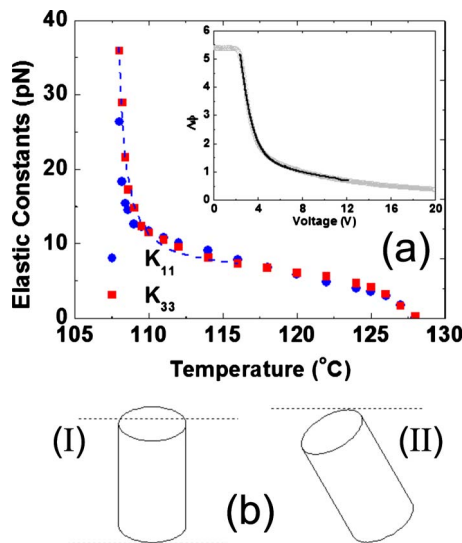
FIG. 3. (Color online) (a) Variation of K_{11} and K_{33} as a function of temperature. Dashed line is a theoretical fit to $K_{33}=K_{33}^0 +A[(T/T_{NS})-1]^{-x}$. (Inset) Retardation as a function of applied voltage at 126 °C. Continuous line is a theoretical fit to Eqs. (1) and (2). (b) (i) Schematic of the splay fluctuations at the onset of short-range smectic order. Note the tilting of the molecule (splay deformation) is associated with a change in the layer spacing in (b)(II).

longitudinal and transverse dipole components mainly due to the azo and ester linkages. The partial suppression of the transverse dipole moment in the nematic phase is made possible by largely unhindered rotations about the long molecular axis. This leads to a positive $\Delta\epsilon$ in the N phase. In the Sm-A phase the dielectric anisotropy is reduced because the rotations about their long axes are more hindered due to the presence of a long side chain. This results in developing a quasimacroscopic transverse dipoles as suggested by Sathyanarayana *et al.* [5]. Further, the increased in-layer dipolar correlation as reported by de Jeu *et al.* [18] has significant contribution in reducing the dielectric anisotropy in the Sm-A phase.

To measure K_{11} and K_{33}, the optical phase difference ($\Delta\phi=2\pi\Delta nd/\lambda$) of the sample was measured as a function of voltage. A typical variation of experimental data $\Delta\phi$ at a temperature 126 °C and the best fit to Eq. (2) are shown in Fig. 3(a). K_{11} was measured directly from the Freedericksz transition as mentioned earlier. The experimental data at higher voltage was fitted to the parametric equations [Eqs. (1) and (2)] to get K_{33} as a fit parameter. The temperature dependent variation of both K_{11} and K_{33} is shown in Fig. 3(a). The variation of K_{33} near T_{NI} is proportional to S^2 and K_{33} increases as the temperature is reduced similar to its variation as in the case of many calamitic liquid crystals, diverging rapidly as the SN transition is approached. Interestingly we find that the temperature dependence of K_{11} is the same as that of K_{33}. The ratio $K_{33}/K_{11}\sim 1$ at all temperatures except very close to the SN transition. This ratio varies from 2 to 6 in case of rodlike molecules (e.g., 8OCB) as the temperature is reduced from the NI to the SN transition. K_{33} shows strong pretransitional divergence as predicted and is given by $K_{33}=K_{33}^0+A[(T/T_{NS})-1]^{-x}$ [19], where K_{33}^0 is the

background nematic contribution and x is the critical exponent. In the present compound $x=1\pm0.09$ which is similar to the value reported for 8CB [10]. It is known that for rigid rodlike molecules $K_{33}/K_{11}\sim L/D$ where L/D is the length to width ratio of the molecule [20], and it is found to decrease when flexible groups are present in the molecules. Using a semiempirical relation for flexible molecules, the ratio K_{33}/K_{11} can be related to the molecular properties and is expressed as [20]: $K_{33}/K_{11}=([1+\Delta-3\Delta'\overline{P_4/P_2}]/([1+\Delta +4\Delta'\overline{P_4/P_2}])$; where $\Delta=(2R^2-2)/(7R^2+20)$, $\Delta'=9(3R^2 -8)/16(7R^2+20)$. $R=(L-D)/D$, where L and D are the length and width of the molecule. Since the molecules have long flexible lateral group, we calculated the radius of gyration along the long axis to estimate their width. It turns out that this width ($\simeq9$ Å) is about a third of the experimentally measured length of the long axis (28.8 Å, discussed below), i.e., $L\simeq3D$. Assuming $\overline{P_4/P_2}$ is small (~0.1) and with $L\simeq3D$ (i.e., $R\simeq2$) and the ratio, $K_{33}/K_{11}\simeq1$ which is close to the experimental value obtained [Fig. 3(a)].

The divergence of K_{11} is a consequence of suppression of splay fluctuations as Sm-A phase is approached. This looks unusual since the splay fluctuations are taken to be compatible with the constant layer spacing requirement of smectics in conventional liquid crystals. However in the present case, the molecule has a long flexible lateral group and is undergoing largely unhindered rotations along the long axis. This seems to modify the aspect ratio of the molecules, effectively making it ~3 (i.e., $L\simeq3D$), depicted as a cylinder in Fig. 3(b)-I. Splay fluctuations involving such objects lead to significant changes in the layer spacing as shown schematically in Fig. 3(b)-II, necessitating relatively large elastic energy. Hence the splay fluctuations are considerably suppressed leading to the observed divergence in K_{11}. Further, compared to more rigid molecules the flexible terminal alkyl chains and long flexible lateral groups have the potential to partially hinder the mutual sliding of the molecules along each other. The consequent close proximity of aromatic cores of neighboring molecules may also be responsible for larger effective width, thus supporting the experimental observations.

Finally we discuss the arrangement of T-shaped molecules in the smectic layers as suggested from the x-ray diffraction measurements. Typical intensity profile as a function of angle ϑ is shown in Fig. 4. Two sharp reflections in the small-angle region with spacing 28.8 Å, 15.1 Å, as well as an additional broad diffuse wide-angle reflection at about 4.6 Å can be seen. Ratio of the two spacings 1: 0.5 clearly indicates a layered structure. Length of different segments of a single molecule was also estimated from energy minimized structure by considering different dihedral angles. The average length of the particular segment, containing three phenyl rings, azo and ester linkages with two terminal alkyl chains, is $L\simeq31$ Å [Fig. 2(a)]. This suggests that L is parallel to the smectic layer normal and the flexible chains are randomly oriented in the plane of the smectic layer as schematically shown in Fig. 4. Slightly lower value of the experimentally measured length (i.e., 28.8 Å), compared to the computed L value (=31 Å) from the energy minimized structure, suggests that the molecules is not fully stretched in the Sm-A phase.

In conclusion, we measured elastic constants K_{11} and K_{33}

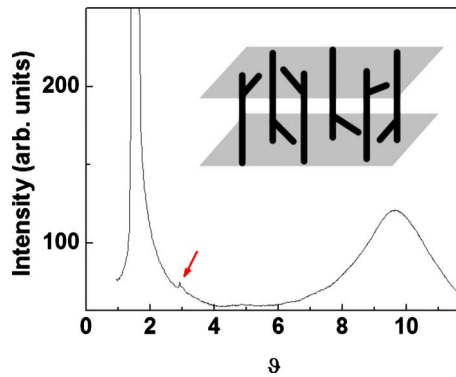FIG. 4. (Color online) X-ray intensity as a function of angle ϑ. Arrow indicates a small second order reflection. (Inset) Schematic arrangement of molecules in the Sm-*A* layer.

as a function of temperature in a liquid crystal with T-shaped molecules exhibiting *both* first order NI and SN transitions. Our measurements show that $K_{33}/K_{11} \sim 1$ and *both* diverge as the Sm-*A* is approached. These results suggest that the length to effective width ratio of the molecule is smaller than that of rigid rodlike molecules due to the presence of long flexible lateral group. Small angle x-ray diffraction and energy minimized structure suggest that the three phenyl rings and two linkages (azo and ester) and two terminal alkyl chains form the long axis. This axis is parallel to the Sm-*A* layer normal and the flexible lateral groups are in the plane. This system may prove to be a convenient medium for testing theoretical models based on one elastic constant approximation. Detailed theoretical investigations can through light to understand the observed divergence of the spay elastic constant of such compounds from the perspective of elastic free energy considerations near the SN transition.

[1] J. I. Jin, J. S. Kim, Y. K. Yun, and W. C. Zin, Mol. Cryst. Liq. Cryst. **308**, 99 (1997) and references therein.

[2] W. S. Bae, J. W. Lee, and J. I. Jin, Liq. Cryst. **28**, 59 (2001); A. Sato and A. Yoshizawa, Ferroelectrics **364**, 1 (2008).

[3] I. Miyake, *et al.*, J. Mater. Chem. **15**, 4688 (2005); S. K. Lee *et al.*, Liq. Cryst. **34**, 935 (2007).

[4] H. Takezoe and Y. Takanishi, J. Appl. Phys. **45**, 597 (2006).

[5] P. Sathyanarayana *et al.*, Phys. Rev. E **81**, 010702(R) (2010).

[6] D. Wiant, J. T. Gleeson, N. Eber, K. Fodor-Csorba, A. Jakli, and T. Toth-Katona, Phys. Rev. E **72**, 041712 (2005); S. Tanaka *et al.*, *ibid.* **77**, 041708 (2008).

[7] J. Harden, B. Mbanga, N. Eber, K. Fodor-Csorba, S. Sprunt, J. T. Gleeson, and A. Jakli, Phys. Rev. Lett. **97**, 157802 (2006).

[8] E. Dorjgotov, K. Fodor-Csorba, J. T. Gleeson, S. Sprunt, and A. Jakli, Liq. Cryst. **35**, 149 (2008).

[9] Oakberg, Proc. SPIE **3121**, 19 (1997).

[10] S. W. Morris, P. Palffy, and D. A. Balzarini, Mol. Cryst. Liq. Cryst. **139**, 263 (1986).

[11] B. Kundu, R. Pratibha, and N. V. Madhusudana, Phys. Rev. Lett. **99**, 247802 (2007).

[12] W. L. McMillan, Phys. Rev. A **6**, 936 (1972).

[13] C. W. Garland and G. Nounesis, Phys. Rev. E **49**, 2964 (1994).

[14] M. E. Huster, K. J. Stine, and C. W. Garland, Phys. Rev. A **36**, 2364 (1987); J. Caerels, C. Glorieux, and J. Thoen, Phys. Rev. E **65**, 031704 (2002).

[15] J. Thoen *et al.*, Liq. Cryst. **2**, 853 (1987).

[16] I. Lelidis, Phys. Rev. Lett. **86**, 1267 (2001).

[17] G. A. Oweimreen and M. A. Morsy, Thermochim. Acta **346**, 37 (2000).

[18] W. H. de Jeu, T. W. Lathouwers, and P. Bordewijk, Phys. Rev. Lett. **32**, 40 (1974).

[19] T. C. Lubensky, J. de Chim. Phys. **80**, 31 (1983); P. G. de Gennes, Mol. Cryst. Liq. Cryst. **21**, 49 (1973).

[20] R. G. Priest, Phys. Rev. A **7**, 720 (1973).